9-2013

Complex reflection coefficients of p- and s-polarized light at the pseudo-Brewster angle of a dielectric–conductor interface

Rasheed M.A. Azzam

University of New Orleans, razzam@uno.edu

Recommended Citation

R. M. A. Azzam, "Complex reflection coefficients of p- and s-polarized light at the pseudo-Brewster angle of a dielectric–conductor interface," J. Opt. Soc. Am. A 30, 1975-1979 (2013)

Complex reflection coefficients of *p*- and *s*-polarized light at the pseudo-Brewster angle of a dielectric–conductor interface

R. M. A. Azzam

Department of Electrical Engineering, University of New Orleans, New Orleans, Louisiana 70148, USA (razzam@uno.edu)

Received July 23, 2013; revised August 15, 2013; accepted August 16, 2013; posted August 16, 2013 (Doc. ID 194457); published September 10, 2013

The complex Fresnel reflection coefficients r_p and r_s of p- and s-polarized light and their ratio $\rho = r_p/r_s$ at the pseudo-Brewster angle (PBA) ϕ_{pB} of a dielectric–conductor interface are evaluated for all possible values of the complex relative dielectric function $\varepsilon = |\varepsilon|\exp(-j\theta) = \varepsilon_r - j\varepsilon_i$, $\varepsilon_i > 0$ that share the same ϕ_{pB}. Complex-plane trajectories of r_p, r_s, and ρ at the PBA are presented at discrete values of ϕ_{pB} from 5° to 85° in equal steps of 5° as θ is increased from 0° to 180°. It is shown that for $\phi_{pB} > 70°$ (high-reflectance metals in the IR) r_p at the PBA is essentially pure negative imaginary and the reflection phase shift $\delta_p = \arg(r_p) \approx -90°$. In the domain of fractional optical constants (vacuum UV or light incidence from a high-refractive-index immersion medium) $0 < \phi_{pB} < 45°$ and r_p is pure real negative ($\delta_p = \pi$) when $\theta = \tan^{-1}(\sqrt{\cos(2\phi_{pB})})$, and the corresponding locus of ε in the complex plane is obtained. In the limit of $\varepsilon_i = 0$, $\varepsilon_r < 0$ (interface between a dielectric and plasmonic medium) the total reflection phase shifts δ_p, δ_s, $\Delta = \delta_p - \delta_s = \arg(\rho)$ are also determined as functions of ϕ_{pB}. © 2013 Optical Society of America

OCIS codes: (120.5700) Reflection; (240.0240) Optics at surfaces; (240.2130) Ellipsometry and polarimetry; (260.0260) Physical optics; (260.3910) Metal optics; (260.5430) Polarization.

http://dx.doi.org/10.1364/JOSAA.30.001975

1. INTRODUCTION

A salient feature of the reflection of collimated monochromatic p (TM)-polarized light at a planar interface between a transparent medium of incidence (dielectric) and an absorbing medium of refraction (conductor) is the appearance of a reflectance minimum at the pseudo-Brewster angle (PBA) ϕ_{pB}. If the medium of refraction is also transparent, the minimum reflectance is zero and ϕ_{pB} reverts back to the usual Brewster angle $\phi_B = \tan^{-1} n = \tan^{-1}\sqrt{\varepsilon_r}$. The PBA ϕ_{pB} is determined by the complex relative dielectric function $\varepsilon = \varepsilon_1/\varepsilon_0 = \varepsilon_r - j\varepsilon_i$, $\varepsilon_i > 0$, where ε_0 and ε_1 are the real and complex permittivities of the dielectric and conductor, respectively, by solving a cubic equation in $u = \sin^2\phi_{pB}$ [1–5]. Measurement of ϕ_{pB} and of reflectance at that angle or at normal incidence enables the determination of complex ε [1,6–9]. It is also possible to determine ε of an optically thick absorbing film from two PBAs measured in transparent ambient and substrate media that sandwich the thick film [10]. Reflection at the PBA has also had other interesting applications [11,12].

For light reflection at any angle of incidence ϕ the complex-amplitude Fresnel reflection coefficients (see, e.g., [13]) of the p and s polarizations are given by

$$r_p = \frac{\varepsilon\cos\phi - (\varepsilon - \sin^2\phi)^{1/2}}{\varepsilon\cos\phi + (\varepsilon - \sin^2\phi)^{1/2}}, \tag{1}$$

$$r_s = \frac{\cos\phi - (\varepsilon - \sin^2\phi)^{1/2}}{\cos\phi + (\varepsilon - \sin^2\phi)^{1/2}}. \tag{2}$$

All possible values of complex $\varepsilon = (\varepsilon_r, \varepsilon_i)$ that share the same ϕ_{pB} are generated by using the following algorithm [8,14]:

$$\varepsilon_r = |\varepsilon|\cos\theta, \qquad \varepsilon_i = |\varepsilon|\sin\theta, \tag{3}$$

$$\begin{aligned} &|\varepsilon| = \ell\cos(\varsigma/3),\\ &\ell = 2u\left(1 - \frac{2}{3}u\right)^{1/2}/(1-u),\\ &\varsigma = \cos^{-1}\left[-(1-u)\cos\theta/\left(1-\frac{2}{3}u\right)^{3/2}\right],\\ &u = \sin^2\phi_{pB},\\ &0 \le \theta \le 180°. \end{aligned} \tag{4}$$

As θ is increased from 0° to 180°, the minimum reflectance $|r_p|_{\min}$ at a given ϕ_{pB} increases monotonically from 0 to 1 [15] and also as is evident in Fig. 1 of Section 2.

In this paper, loci of all possible values of complex $r_p = |r_p|\exp(j\delta_p)$, $r_s = |r_s|\exp(j\delta_s)$, and $\rho = r_p/r_s = |\rho|\exp(j\Delta)$ at the PBA are determined at discrete values of ϕ_{pB} from 5° to 85° in equal steps of 5° and as $\theta = -\arg(\varepsilon)$ covers the full range $0° \le \theta \le 180°$. These results are presented in Sections 2, 3, and 4, respectively, and lead to interesting conclusions. In particular, questions related to phase shifts that accompany the reflection of p- and s-polarized light at the PBA (e.g., [12]) are settled. Section 5 summarizes the essential conclusions of this paper.

2. COMPLEX REFLECTION COEFFICIENT OF THE p POLARIZATION AT THE PBA

Figure 1 shows the loci of complex r_p as θ increases from 0° to 180° at constant values of ϕ_{pB} from 5° to 85° in equal steps of 5°. All constant-ϕ_{pB} contours begin at the origin O ($\theta = 0$) as a common point, that represents zero reflection at an ideal Brewster angle, and end on the 90° arc of the unit circle in the third quadrant (shown as a dotted line) that represents total reflection $|r_p| = 1$ at $\theta = 180°$ ($\varepsilon_i = 0, \varepsilon_r < 0$). A quick conclusion from Fig. 1 is that for $\phi_{pB} > 70°$ (high-reflectance metals) r_p at the PBA is essentially pure negative imaginary, and $\delta_p \approx -90°$.

In Fig. 1 the constant-ϕ_{pB} contours of r_p for $0 < \phi_{pB} < 45°$ spill over into a limited range of the second quadrant of the complex plane and each contour intersects the negative real axis. In Appendix A it is shown that θ at the point of intersection, where $\delta_p = \arg(r_p) = \pi$, is given by the remarkably simple formula

$$\theta(\delta_p = \pi) = \tan^{-1}\left(\sqrt{\cos(2\phi_{pB})}\right). \quad (5)$$

A graph of this function of Eq. (5) is shown in Fig. 2.

The locus of complex ε such that $\delta_p = \arg(r_p) = \pi$ at the PBA [as determined by Eqs. (3)–(5)] falls in the domain of fractional optical constants and is shown in Fig. 3. The end points (0, 0) and (1, 0) of this trajectory correspond to $\phi_{pB} = 0$ and 45°, respectively. At $\varepsilon = (0.6, 0.3)$, a point that falls exactly on the curve very near to its peak, $\phi_{pB} = 37.761°$.

For small PBAs, $\phi_{pB} \leq 5°$, the upper limit on $|\varepsilon|$ is calculated from ℓ of Eq. (4), $|\varepsilon| = \ell \leq 0.0153$, and represents the domain of so-called epsilon-near-zero (ENZ) materials [16].

Negative real values of ε at $\theta = 180°$ [14] are given by

$$\varepsilon = \varepsilon_r = -\frac{1}{2}\tan^2\phi_{pB}[1 + (9 - 8\sin^2\phi_{pB})^{1/2}] \quad (6)$$

and represent light reflection at an ideal dielectric–plasmonic medium interface. The corresponding total reflection phase shift δ_p as $\theta \to 180°$ (at the end point of each contour in Fig. 1)

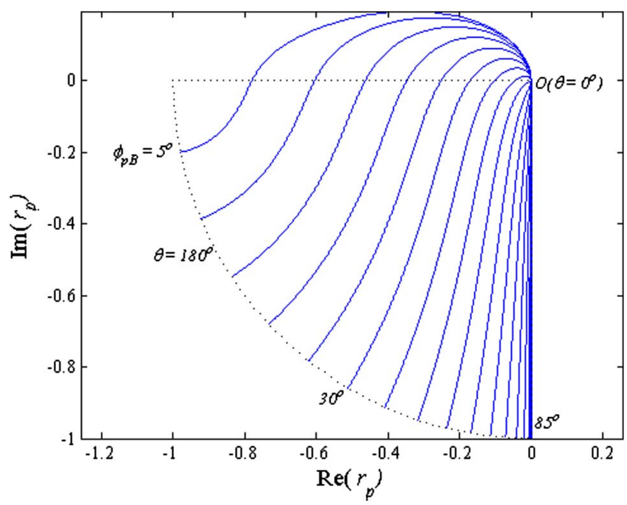

Fig. 1. Complex-plane trajectories of r_p at discrete values of the PBA ϕ_{pB} from 5° to 85° in equal steps of 5° as $\theta = -\arg(\varepsilon)$ covers the full range $0° \leq \theta \leq 180°$.

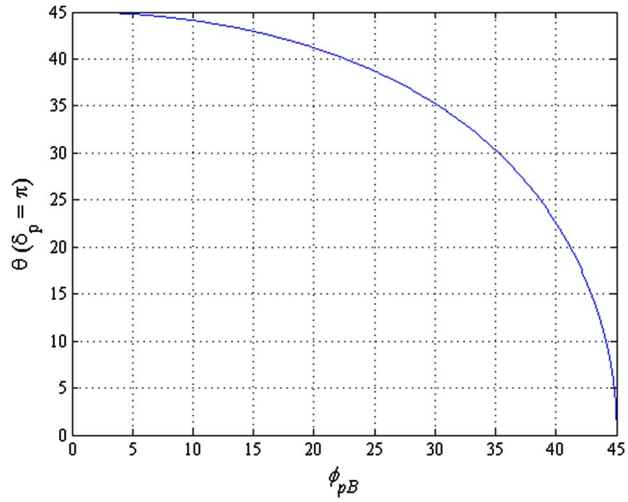

Fig. 2. Graph of the function of Eq. (5). Both ϕ_{pB} and θ are in degrees.

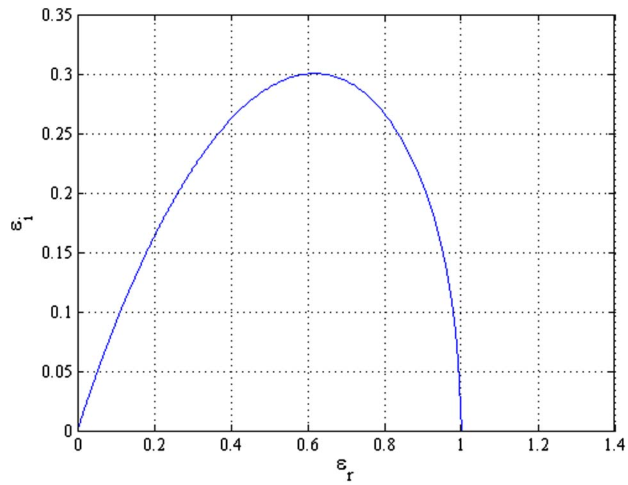

Fig. 3. Locus of all possible values of complex ε such that $\delta_p = \arg(r_p) = \pi$ at the PBA.

is obtained from Eqs. (1) and (6) and is plotted as a function of ϕ_{pB} in Fig. 4. In Fig. 4 δ_p increases monotonically from −180° to −90° as ϕ_{pB} increases from 0° to 90°. The initial rise of δ_p with respect to ϕ_{pB} is linear for $\phi_{pB} < 20°$ and then transitions to saturation at $\phi_{pB} > 70°$, in accord with Fig. 1.

In Fig. 5 δ_p is plotted as a function of θ for ϕ_{pB} from 10° to 40° in equal steps of 10°. Vertical transitions from +180° to −180° are located at θ values that agree with Eq. (5).

Another family of δ_p-versus-θ curves for ϕ_{pB} from 45° to 85° in equal steps of 5° is shown in Fig. 6. For $\phi_{pB} > 45°$ the δ_p-versus-θ curve first exhibits a minimum then reaches saturation as $\theta \to 180°$. The saturated value of δ_p is a function of ϕ_{pB} and is shown in Fig. 4.

3. COMPLEX REFLECTION COEFFICIENT OF THE s POLARIZATION AT THE PBA

Figure 7 shows the loci of complex r_s as θ increases from 0° to 180° at discrete values of ϕ_{pB} from 5° to 85° in equal steps of 5°. All curves start on the real axis at $\theta = 0$, $r_s = \cos(2\phi_{pB})$, which is the s amplitude reflectance at the Brewster angle of a

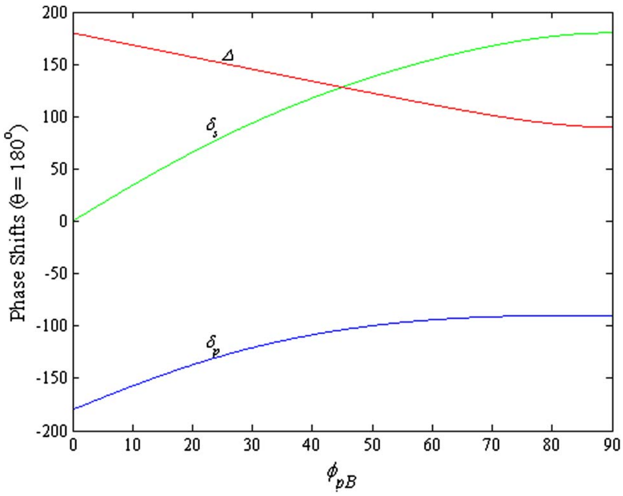

Fig. 4. Total reflection phase shifts δ_p, δ_s, and $\Delta = \delta_p - \delta_s + 360°$ at the interface between a dielectric and plasmonic medium in the limit as $\theta \to 180°$ ($\varepsilon_i = 0, \varepsilon_r < 0$) are plotted as a functions of ϕ_{pB}. All angles are in degrees.

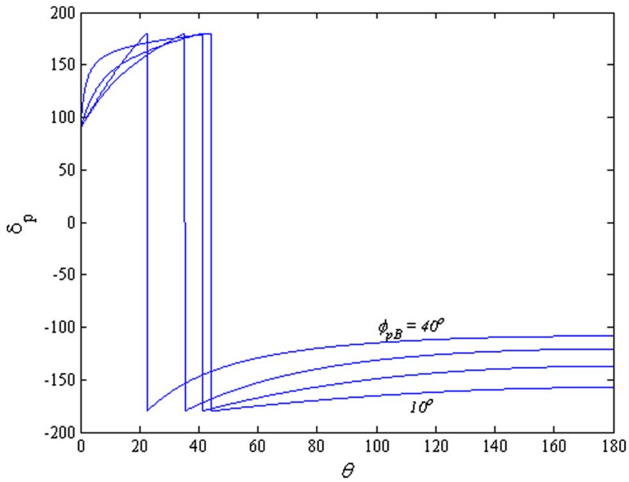

Fig. 5. Family of δ_p versus θ curves for ϕ_{pB} from 10° to 40° in equal steps of 10°. Both θ and δ_p are in degrees.

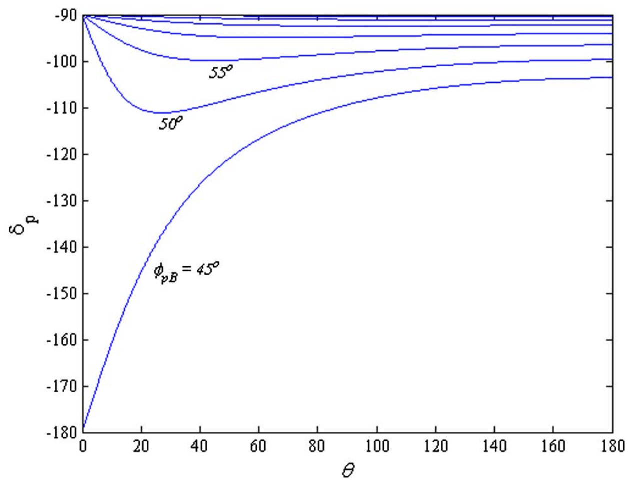

Fig. 6. Family of δ_p versus θ curves for ϕ_{pB} from 45° to 85° in equal steps of 5°. Both θ and δ_p are in degrees.

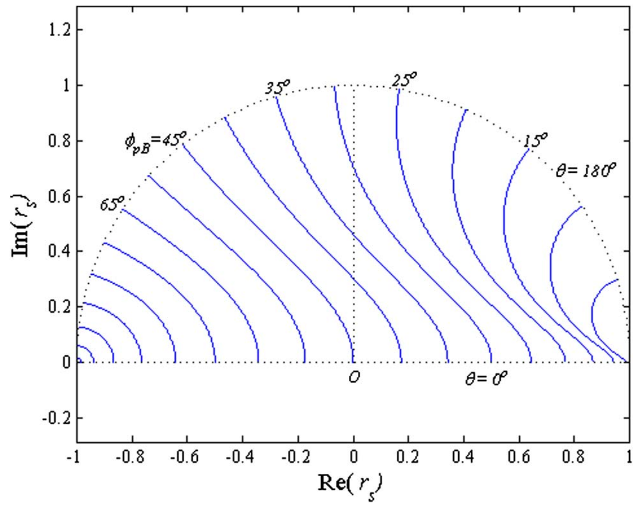

Fig. 7. Complex-plane contours of r_s at discrete values of the PBA ϕ_{pB} from 5° to 85° in equal steps of 5° as $\theta = -\arg(\varepsilon)$ covers the full range from 0° to 180°.

dielectric–dielectric interface [17], and terminate on the upper half of the unit circle (dotted line) that represents total reflection $r_s = \exp(j\delta_s)$ at $\theta = 180°$ ($\varepsilon_i = 0, \varepsilon_r < 0$). The associated total reflection phase shift δ_s along the dotted semicircle is a function of ϕ_{pB} as shown in Fig. 4.

Although we are locked on the PBA, all possible values of complex r_s (within the upper half of the unit circle) are generated at that angle. This is not the case of complex r_p at the PBA (Fig. 1) which is squeezed mostly in the third quadrant of the unit circle. Recall that the unconstrained domain of r_p for light reflection at all dielectric–conductor interfaces is on and inside the full unit circle [17].

4. RATIO OF COMPLEX REFLECTION COEFFICIENTS OF THE *p* AND *s* POLARIZATIONS AT THE PBA

The ratio of complex p and s reflection coefficients, also known as the ellipsometric function $\rho = \tan\psi \exp(j\Delta)$ [13], is obtained from Eqs. (1) and (2) as

$$\rho = r_p/r_s = \frac{\sin\phi\tan\phi - (\varepsilon - \sin^2\phi)^{1/2}}{\sin\phi\tan\phi + (\varepsilon - \sin^2\phi)^{1/2}}. \qquad (7)$$

Figure 8 shows loci of complex ρ as θ increases from 0° to 180° at constant values of ϕ_{pB} from 5° to 85° in equal steps of 5°. All contours begin at the origin O (as a common point that represents the ideal Brewster-angle condition of $r_p = 0$ at $\theta = 0$), then fan out and terminate on the 90° arc of the unit circle in the second quadrant of the complex plane (dotted line), so that $\rho = \exp(j\Delta)$ at $\theta = 180°$ ($\varepsilon_i = 0, \varepsilon_r < 0$). The differential reflection phase shift $\Delta = \delta_p - \delta_s + 360°$ at $\theta = 180°$ decreases monotonically from 180° to 90° as ϕ_{pB} increases from 0° to 90° as shown in Fig. 4.

5. SUMMARY

The Fresnel complex reflection coefficients r_p, r_s and their ratio $\rho = r_p/r_s$ are evaluated at the PBA ϕ_{pB} of a dielectric–conductor interface for all possible values of the complex relative dielectric function $\varepsilon = |\varepsilon|\exp(-j\theta) = \varepsilon_r - j\varepsilon_i$, $\varepsilon_i > 0$.

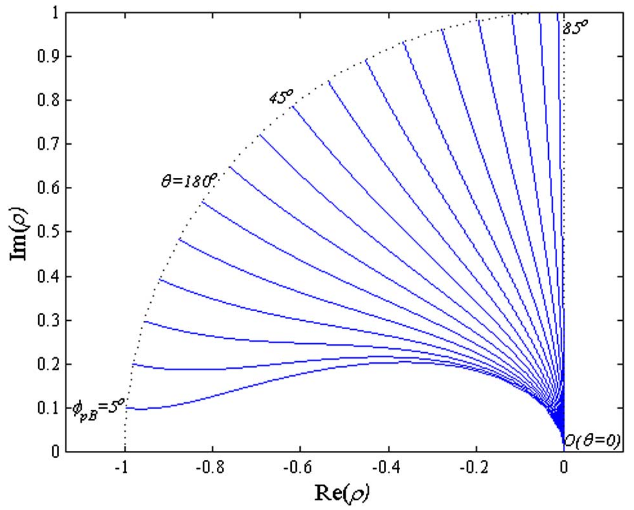

Fig. 8. Complex-plane trajectories of the ratio $\rho = r_p/r_s$ at discrete values of the PBA ϕ_{pB} from 5° to 85° in equal steps of 5° as $\theta = -\arg(\varepsilon)$ covers the full range $0° \le \theta \le 180°$.

Complex-plane loci of r_p, r_s, and ρ at the PBA are obtained at discrete values of ϕ_{pB} from 5° to 85° in equal steps of 5° and as θ increases from 0° to 180°; these are presented in Figs. 1, 7, and 8, respectively. The reflection phase shift δ_p of the p polarization at the PBA is plotted as function of θ in Figs. 5 and 6 for two different sets of ϕ_{pB}. For $\phi_{pB} > 70°$ (e.g., high-reflectance metals in the IR), r_p at the PBA is essentially pure negative imaginary and $\delta_p = \arg(r_p) \approx -90°$. In the domain of fractional optical constants (vacuum UV or light incidence from a high-refractive-index immersion medium) $0° < \phi_{pB} < 45°$, and r_p is pure real negative ($\delta_p = \pi$) at $\theta = \tan^{-1}(\sqrt{\cos(2\phi_{pB})})$. The associated locus of complex ε is shown in Fig. 3. Finally, the total reflection phase shifts δ_p, δ_s, $\Delta = \arg(\rho)$ at an ideal dielectric–plasmonic medium interface ($\varepsilon_i = 0, \varepsilon_r < 0$), are shown as functions of ϕ_{pB} in Fig. 4.

APPENDIX A

By setting $\varepsilon_r = x$ and $\varepsilon_i = y$, the Cartesian equation of a constant-ϕ_{pB} contour (a cardioid [8]) takes the form [10]

$$y^2 = a + (a^2 - bx)^{1/2} - x^2, \tag{A1}$$

$$a = u^2(1.5 - u)/(1 - u)^2, b = u^3/(1 - u)^2, u = \sin^2 \phi_{pB}. \tag{A2}$$

The locus of complex ε such that $\delta_p = \arg(r_p) = \pi$ at a given angle of incidence $\phi = \sin^{-1}\sqrt{u}$ is a circle [18]

$$y^2 = 2ux - x^2. \tag{A3}$$

Equations (A1) and (A3) are satisfied simultaneously if their right-hand sides are equal; this gives

$$(a^2 - bx)^{1/2} = 2ux - a. \tag{A4}$$

By squaring both sides of Eq. (A4) we obtain

$$4u^2x^2 = (4au - b)x. \tag{A5}$$

Equation (A5) is obviously satisfied when $x = 0$, and from Eq. (A3) one gets $y = 0$ and $\varepsilon = 0$. The more significant solution of Eq. (A5) is

$$x = (4au - b)/(4u^2). \tag{A6}$$

Substitution of a and b from Eq. (A2) in Eq. (A6) leads to the simple result

$$x = u/(1 - u). \tag{A7}$$

The associated value of y is then obtained from Eq. (A3) as

$$y = u\sqrt{1 - 2u}/(1 - u). \tag{A8}$$

The angle $\theta = \arg(\varepsilon)$ is determined from Eqs. (A7) and (A8) by

$$\tan\theta = y/x = \sqrt{1 - 2u}. \tag{A9}$$

Finally, substitution of $u = \sin^2\phi_{pB}$ in Eq. (A9) gives

$$\theta(\delta_p = \pi) = \tan^{-1}\left(\sqrt{\cos(2\phi_{pB})}\right). \tag{A10}$$

This completes the proof of Eq. (5).

REFERENCES

1. S. P. F. Humphreys-Owen, "Comparison of reflection methods for measuring optical constants without polarimetric analysis, and proposal for new methods based on the Brewster angle," Proc. Phys. Soc. London **77**, 949–957 (1961).
2. H. B. Holl, "Specular reflection and characteristics of reflected light," J. Opt. Soc. Am. **57**, 683–690 (1967).
3. G. P. Ohman, "The pseudo-Brewster angle," IEEE Trans. Antennas Propag. **25**, 903–904 (1977).
4. R. M. A. Azzam, "Maximum minimum reflectance of parallel-polarized light at interfaces between transparent and absorbing media," J. Opt. Soc. Am. **73**, 959–962 (1983).
5. S. Y. Kim and K. Vedam, "Analytic solution of the pseudo-Brewster angle," J. Opt. Soc. Am. A **3**, 1772–1773 (1986).
6. T. E. Darcie and M. S. Whalen, "Determination of optical constants using pseudo-Brewster angle and normal-incidence reflectance," Appl. Opt. **23**, 1130–1131 (1984).
7. Y. Lu and A. Penzkofer, "Optical constants measurements of strongly absorbing media," Appl. Opt. **25**, 221–225 (1986).
8. R. M. A. Azzam and E. Ugbo, "Contours of constant pseudo-Brewster angle in the complex ε plane and an analytical method for the determination of optical constants," Appl. Opt. **28**, 5222–5228 (1989).
9. M. A. Ali, J. Moghaddasi, and S. A. Ahmed, "Optical properties of cooled rhodamine B in ethanol," J. Opt. Soc. Am. B **8**, 1807–1810 (1991).
10. R. M. A. Azzam, "Analytical determination of the complex dielectric function of an absorbing medium from two angles of incidence of minimum parallel reflectance," J. Opt. Soc. Am. A **6**, 1213–1216 (1989).
11. I. H. Campbell and P. M. Fauchet, "Temporal reshaping of ultrashort laser pulses after reflection from GaAs at Brewster's angle," Opt. Lett. **13**, 634–636 (1988).
12. Y. Lv, Z. Wang, Y. Jin, M. Cao, L. Han, P. Zhang, H. Li, H. Gao, and F. Li, "Spin polarization separation of light reflected at Brewster angle," Opt. Lett. **37**, 984–986 (2012).
13. R. M. A. Azzam and N. M. Bashara, *Ellipsometry and Polarized Light* (North-Holland, 1987).
14. R. M. A. Azzam and A. Alsamman, "Plurality of principal angles for a given pseudo-Brewster angle when polarized light is reflected at a dielectric-conductor interface," J. Opt. Soc. Am. A **25**, 2858–2864 (2008).

15. R. M. A. Azzam and E. Ugbo, "Angular range for reflection of p-polarized light at the surface of an absorbing medium with reflectance below that at normal incidence," J. Opt. Soc. Am. A **19**, 112–115 (2002).
16. A. Alù, M. G. Silveirinha, A. Salandrino, and N. Engheta, "Epsilon-near-zero metamaterials and electromagnetic sources: tailoring the radiation phase pattern," Phys. Rev. B **75**, 155410 (2007).
17. R. M. A. Azzam, "Direct relation between Fresnel's interface reflection coefficients for the parallel and perpendicular polarizations," J. Opt. Soc. Am. **69**, 1007–1016 (1979).
18. R. M. A. Azzam, "Reflection of an electromagnetic plane wave with 0 or π phase shift at the surface of an absorbing medium," J. Opt. Soc. Am. **69**, 487–488 (1979).